ELSEVIER

Journal of Computational and Applied Mathematics 126 (2000) 233–254

JOURNAL OF COMPUTATIONAL AND APPLIED MATHEMATICS

www.elsevier.nl/locate/cam

# A mathematical model for the dissolution of particles in multi-component alloys

F.J. Vermolen[a,b], C. Vuik[c]

[a] *CWI, P.O. Box 94079, 1090 GB, Amsterdam, Netherlands*

[b] *Laboratory for Materials Science, Delft University of Technology, Rotterdamseweg 137, 2628 AL Delft, Netherlands*

[c] *Faculty of Technical Mathematics and Informatics, Delft University of Technology, P.O. Box 5031, 2600 GA Delft, Netherlands*

Received 20 April 1999; received in revised form 15 September 1999

**Abstract**

Dissolution of stoichiometric multi-component particles is an important process occurring during the heat treatment of as-cast aluminum alloys prior to hot extrusion. A mathematical model is proposed to describe such a process. In this model equations are given to determine the position of the particle interface in time, using a number of diffusion equations which are coupled by nonlinear boundary conditions at the interface. This problem is known as a vector valued Stefan problem. A necessary condition for existence of a solution of the moving boundary problem is proposed and investigated using the maximum principle for the parabolic partial differential equation. Furthermore, for an unbounded domain and planar co-ordinates an asymptotic approximation based on self-similarity is derived. The asymptotic approximation is used to gain insight into the influence of all components on the dissolution. Subsequently, a numerical treatment of the vector valued Stefan problem is described. The numerical solution is compared with solutions obtained by the analytical methods. Finally, an example is shown. 

*MSC:* 35A35; 35R35; 65M06; 80A22

*Keywords:* Self-similar solution; Vector-valued Stefan problem; Alloy homogenization; Finite differences; Newton–Raphson method

## 1. Introduction

Heat treatment of metals is often necessary to optimize their mechanical properties. During the heat treatment the metallurgical state of the alloy changes. This change can either involve the phases being present or the morphology of the various phases. Whereas the equilibrium phases can be predicted

*E-mail addresses:* fredv@cwi.nl (F.J. Vermolen), c.vuik@math.tudelft.nl (C. Vuik)

0377-0427/00/$ - see front matter 
PII: S0377-0427(99)00355-6

quite accurately from the thermodynamic models, until recently there were no general models for microstructural changes nor general models for the kinetics of these changes. In the latter cases both the initial morphology and the transformation mechanisms have to be specified explicitly. One of these processes that is amenable to modeling is the dissolution of secondary (multi-component) phase particles in an alloy with a given initial composition.

To describe this particle dissolution in solid media several physical models for binary alloys have been developed, incorporating the effects of long-distance diffusion [43,2,30] and nonequilibrium conditions at the interface [25,1,32,40]. These articles did not cover the technologically important dissolution of stoichiometric multi-component particles in multi-component alloys.

Phase transformations in steels have been studied in [14,38]. Reiso et al. [28] investigated the dissolution of $Mg_2Si$-particles in aluminum alloys mainly experimentally. They compared their results to a simple dissolution model valid for dissolution in infinite media. Hubert [16] studied the dissolution and growth of second-phase particles, consisting of AlN in an iron-based ternary alloy. His analysis was carried out to predict the size of second-phase particles during hot-rolling of steel. His model was based on similar physical assumptions as in this paper. However, his approach was purely numerical. The numerical method of [16] differs significantly from the method used in this paper and is applicable to compounds of maximally two alloying elements. Vermolen et al. [34] proposed a numerical method, based on a Newton–Raphson iteration for the computation of the dissolution in ternary alloys. They partly analyzed the properties of this Stefan problem in terms of existence, uniqueness and monotonicity of the solution and well-posedness of the model [35,34]. Some physical implications of the model are described in [36] and applications in aluminum and steel industry are given in, respectively, [12] and [16].

The present work concerns a Stefan problem in which the growth or dissolution of the particle is determined by diffusion of several chemical elements in the primary phase. In Section 2 a mathematical model is given for particle dissolution. The resulting model is a vector-valued Stefan Problem. A number of properties of a scalar Stefan problem is given in Section 3. One of these properties leads to a necessary condition for existence. This condition is used to select a unique solution for a vector-valued Stefan problem. In Section 4 a self-similar solution is presented. A limit solution is investigated in Section 5. This limit solution turns out to be very usefull for many cases in metallurgy. After outlining a numerical method in Section 6, a number of experiments are considered in Section 7. Finally, we give some conclusions.

## 2. A model of dissolution in multi-component alloys

Various particle geometries (planar, cylindrical or spherical) are observed in practice. In this paragraph a cylindrical geometry is considered. The alloy is divided into cells, such that there is no transport between different cells. In some alloys, segregation has also occurred at the cell boundary. Therefore, we consider an angular geometry where the particle is denoted by index $L$ and the segregation layer by index $R$ (see Fig. 1). In our model it is possible that the particle and segregation layer have a different chemical compound.

Consider $n+1$ chemical species denoted by $Sp_i,\ i \in \{1,\ldots,n+1\}$. For the present we assume that all cells have the same geometry and size. The dissolving particles have the same geometry as the cell and have equal size in each cell. It is assumed that the overall concentrations of $Sp_i,\ i \in \{1,\ldots,n\}$

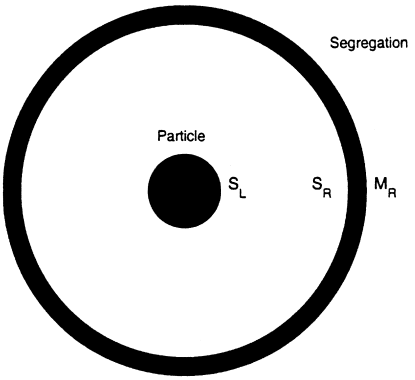


Fig. 1. The geometry (cylindrical) used in the model.

are small with respect to the concentration of component $Sp_{n+1}$. The concentrations are written as $c_i$ (mol/m$^3$), $i \in \{1,\dots,n\}$. At a given temperature the initial concentrations in the $Sp_{n+1}$-rich phase are equal to $c_i^0$, $i \in \{1,\dots,n\}$. The composition of the components in the particle and segregation layer are denoted by $c_{i,k}^{\text{part}}$, $i \in \{1,\dots,n\}$, $k \in \{L,R\}$. We assume these concentrations to be fixed. The interface concentrations $c_{i,k}^{\text{sol}}$ are variant.

We consider a one-dimensional problem. The geometry is given by $\Omega(t) = \{r \in \mathbb{R} \,|\, M_L \leqslant S_L(t) < r < S_R(t) \leqslant M_R\}$, $t \in [0,T]$ where $T$ is an arbitrary positive number. In some applications there is a time $t_L$ and $t_R$ such that respectively $S_L(t) = M_L, t \geqslant t_L$ and $S_R(t) = M_R, t \geqslant t_R$, so the particle or the segregation is dissolved then. For the determination of $c_i$ we use the multi-component version of Fick's second law (see [36,26, p. 160]). For simplicity we assume that all species diffuse independently, and that the diffusion coefficients $\mathbb{D}_i$, $i \in \{1,\dots,n\}$ (m$^2$/s) are constant. The resulting equations are

$$\frac{\partial c_i}{\partial t} = \frac{\mathbb{D}_i}{r^a}\frac{\partial}{\partial r}\left(r^a \frac{\partial c_i}{\partial r}\right), \quad r \in \Omega(t),\ t \in (0,T],\ i \in \{1,\dots,n\}, \tag{1}$$

where $a$ is a geometric parameter, which equals 0,1, or 2 for, respectively, a planar, a cylindrical, or a spherical geometry. Note that $M_L$ should be nonnegative for $a \neq 0$. Initial conditions are

$$c_i(r,0) = c_i^0(r), \quad r \in \Omega(0),\ i \in \{1,\dots,n\}, \tag{2}$$

where $c_i^0$ are given nonnegative functions. When a moving boundary becomes fixed (i.e. $S_k = M_k, k \in \{L,R\}$), we assume that there is no flux through the boundary, so

$$\frac{\partial c_i}{\partial r}(M_k,t) = 0, \quad \text{for } t \geqslant t_k,\ i \in \{1,\dots,n\},\ k \in \{L,R\}. \tag{3}$$

In the following we assume that the particle contains $n_L$ chemical species with indices in $\Phi_L \subset \{1,\dots,n+1\}$ and the segregation contains $n_R$ chemical species with indices in $\Phi_R \subset \{1,\dots,n+1\}$. The complement of $\Phi_k$ is defined as $\Phi_k^c = \{1,\dots,n+1\} \setminus \Phi_k$. On the moving boundaries the following conditions are used:

$$\frac{\partial c_i}{\partial r}(S_k(t),t) = 0, \quad t \in [0,T],\ i \in \Phi_k^c,\ k \in \{L,R\} \tag{4}$$

and we use the following definition for ease of notation:

$$c_{i,k}^{\mathrm{sol}}(t) := c_i(S_k(t), t), \quad t \in [0, t_k],\ i \in \Phi_k,\ k \in \{L, R\}. \tag{5}$$

So $2 + n_L + n_R$ unknown quantities remain: $S_k(t)$, and $c_{i,k}^{\mathrm{sol}}(t)$, $i \in \Phi_k$, $k \in \{L, R\}$. To obtain a unique solution $2 + n_L + n_R$ boundary conditions are necessary. The chemical compositions of the particle and segregation are given by:

$$\prod_{i \in \Phi_k} (Sp_i)_{m_{i,k}}, \quad k \in \{L, R\}.$$

As an example of our notation consider the dissolution of an $Mg_2Si$ particle in an Al-rich phase. Then $Sp_1 = \mathrm{Mg}$, $Sp_2 = \mathrm{Si}$ and $Sp_3 = \mathrm{Al}$. The values of $m_{1,L}$ and $m_{2,L}$ are 2, 1 respectively, and $n = 2$. We assume that the particle and segregation are stoichiometric, which means that the concentrations $c_{i,k}^{\mathrm{part}}$ are constant. Using the Gibbs free energy of the stoichiometric compound we get [36,18]

$$\prod_{i \in \Phi_k} (c_{i,k}^{\mathrm{sol}}(t))^{m_{i,k}} = K_k, \quad t \in (0, t_k),\ k \in \{L, R\}. \tag{6}$$

Note that these boundary conditions are unusual in Stefan problems. The balance of atoms and the constant composition of the particle and segregation lead to the following equations for the moving boundary positions:

$$(c_{i,k}^{\mathrm{part}} - c_{i,k}^{\mathrm{sol}}(t)) \frac{\mathrm{d}S_k}{\mathrm{d}t}(t) = \mathbb{D}_i \frac{\partial c_i}{\partial r}(S_k(t), t), \quad t \in (0, t_k],\ i \in \Phi_k,\ k \in \{L, R\}. \tag{7}$$

Condition (7) implies

$$\frac{\mathbb{D}_i}{c_{i,k}^{\mathrm{part}} - c_{i,k}^{\mathrm{sol}}(t)} \frac{\partial c_i}{\partial r}(S_k(t), t) = \frac{\mathbb{D}_j}{c_{j,k}^{\mathrm{part}} - c_{j,k}^{\mathrm{sol}}(t)} \frac{\partial c_j}{\partial r}(S_k(t), t), \quad i, j \in \Phi_k,\ k \in \{L, R\}. \tag{8}$$

The moving boundary problem given by Eqs. (1)–(7) is known as a vector-valued Stefan problem. We define the space $Q$ as $Q := \{(r, t) \mid r \in \Omega(t), t \in (0, T)\}$ and we look for solutions of the Stefan problem with the following properties: $S_k \in C^1(0, t_k]$ and $c_i \in C^{2,1}(Q) \cap C(\bar{Q})$. When $c_i^0(S_k(0)) \neq c_i^{\mathrm{sol}}(0)$, $i \in \{1, \ldots, n\}$, then $c_i$ cannot be required to be continuous in $(S_k(0), 0)$. In these points, we require

$$\begin{aligned} \min\{c_i^0(S_k(0)), c_i^{\mathrm{sol}}(0)\} &= \liminf_{\substack{(r,t) \in Q \\ (r,t) \to (S_k(0), 0)}} c_i(r, t) \leqslant \limsup_{\substack{(r,t) \in Q \\ (r,t) \to (S_k(0), 0)}} c_i(r, t) \\ &= \max\{c_i^0(S_k(0)), c_i^{\mathrm{sol}}(0)\}, \end{aligned} \tag{9}$$

compare Friedman [13].

There are some differences between the dissolution in a binary alloy and in a multi-component alloy. In the first place, $n$ diffusion equations have to be solved, which are coupled through conditions (5)–(7) on the moving boundaries. Secondly, the problems are nonlinear due to the balance of atoms on $S_L, S_R$, both in the binary and the multi-component case. However, in the mathematical model for a multi-component alloy an extra nonlinearity occurs in Eq. (6). For a recent book where Stefan problems are considered we refer to [37, see for instance p. 132 (2.5), (2.9)]. Survey papers and books on the Stefan problem are [10,15,20,8,21,5].

## 3. Properties of the scalar $d$-dimensional Stefan problem

Before we tackle the vector valued Stefan problem, we briefly analyze the scalar Stefan problem. First the maximum principle is formulated. Using this maximum principle the ill-posedness of a Stefan problem is discussed. It is shown here that under some conditions no solution exists for the Stefan problem which we consider here. The properties and solution of the Stefan problem are first discussed for the case of one diffusing element, therefore the subscript for the index of the alloying element is omitted.

For completeness, we pose the general multi-dimensional scalar Stefan problem. Diffusion of a chemical element takes place in the primary phase domain, $\Omega(t) \subset \mathbb{R}^d$. This domain encloses and/or is enclosed by the particle, of which the domain is denoted by $P(t)$. The initial concentration in $\Omega(0)$ is given by $c(\underline{r}, 0) = c^0, \underline{r} \in \Omega(0)$. For the concentration, we have in $\Omega(t)$:

$$\frac{\partial c}{\partial t} = \mathbb{D}\nabla(\nabla c), \quad \underline{r} \in \Omega(t),\ t \in (0, T]. \tag{10}$$

For the concentration inside the particle, $P(t)$, we have

$$c(\underline{r}, t) = c^{\text{part}}, \quad \underline{r} \in P(t),\ t \in (0, T]. \tag{11}$$

The boundary condition at the moving boundary ($S(t) = \bar{\Omega}(t) \cap \bar{P}(t)$) is

$$c(\underline{r}, t) = c^{\text{sol}}, \quad \underline{r} \in S(t),\ t \in (0, T],$$

and the normal component of the velocity of the moving boundary, $v_v(t)$, is given by

$$(c^{\text{part}} - c^{\text{sol}})v_v(t) = \mathbb{D}\frac{\partial c}{\partial v}, \quad \underline{r} \in S(t),\ t \in (0, T]. \tag{12}$$

At the fixed boundary, $\Gamma := \partial\Omega \setminus S(t)$, we have an homogeneous Neumann condition, with $v$ defined as the outward normal

$$\frac{\partial c}{\partial v} = 0, \quad \underline{r} \in \Gamma,\ t \in (0, T].$$

In this section $c^{\text{part}}, c^{\text{sol}}$ and $c^0$ are assumed to be constant. We will now summarize some basic properties of this scalar Stefan problem.

### 3.1. The maximum principle for the diffusion equation

The Stefan problem is formed by the diffusion equation and a displacement equation for the moving boundary. The solution of the diffusion equation with the above requirements is unique and satisfies a maximum principle:

*Maximum principle*

Suppose $c$ satisfies the inequality

$$\nabla^2 c - \frac{\partial c}{\partial t} \geqslant 0, \quad \underline{r} \in \Omega(t),\ t \in (0, T], \tag{13}$$

then a local maximum has to occur at the boundaries, or at $t = 0$ (the initial condition). Suppose that a local maximum occurs at the point $P$ on $S$ or $\Gamma$. If $\partial/\partial v$ denotes the derivative in an outward direction from $\Omega(t)$, then $\partial c/\partial v > 0$ at $P$.

This statement is referred to as the maximum principle and has been proved by Protter and Weinberger for a general parabolic operator (see [27, pp. 168, 170]). For an unbounded domain see [39, Lemma 2.4., p. 18]. This principle can also be applied for local minima (and $\partial c/\partial v < 0$) when the inequality in (13) is reversed. The principle thus requires the global extremes of a solution to the diffusion equation to occur either at the boundaries $S(t)$, $\Gamma$ or at $t = 0$.

From the Stefan condition (12), one can deduce immediately that the normal component of the interface velocity, $v_v$ has to satisfy

$$v_v(t)(c^{\text{part}} - c^{\text{sol}})\frac{\partial c}{\partial v}(\underline{r}, t) > 0, \quad \forall \underline{r} \in S(t),\ t \in (0, T],\ c^{\text{part}} \neq c^{\text{sol}} \neq c^0, \tag{14}$$

note that $\partial c/\partial v \neq 0$ due to the maximum principle and $c^{\text{sol}} \neq c^0$.

### 3.2. A necessary condition for existence of a solution for the Stefan problem

We will analyze the existence of a solution for a class of Stefan problems. Inequality (14) will be used in the proof of the existence proposition. First we introduce the following definition.

**Definition 3.1.** A solution of the Stefan problem is called conserving if the solution satisfies

$$\int_{\Omega(t)\cup P(t)} (c(\underline{r}, t) - c^0)\,\mathrm{d}V = (c^{\text{part}} - c^0)\int_{P(0)} \mathrm{d}V, \quad \forall t \in (0, T]. \tag{15}$$

Note that $c(\underline{r}, t) = c^{\text{part}}$, $\underline{r} \in P(t)$, $t \in (0, T]$. This definition states that the total amount of the chemical element remains constant in time. Using the Gauss divergence theorem, it can be proven that if the solution is conserving (i.e. (15) holds), the following statement holds: if $\partial c/\partial v(\underline{r}, t) = 0$, for all $\underline{r} \in \Gamma, t \in (0, T]$ then

$$(c^{\text{part}} - c^{\text{sol}})v_v(t) = \mathbb{D}\frac{\partial c(\underline{r}, t)}{\partial v} \quad \text{for all } \underline{r} \in S(t),\ t \in (0, T]. \tag{16}$$

Now, we formulate a proposition about the nonexistence of a conserving solution.

**Proposition 3.1.** *The Stefan problem has no conserving solution if*

$$(c^{\text{part}} - c^0)(c^{\text{part}} - c^{\text{sol}}) \leqslant 0 \quad \textit{and} \quad c^{\text{sol}} \neq c^0 \textit{ with } c^{\text{part}}, c^{\text{sol}}, c^0 \in \mathbb{R}^+ \cup \{0\}.$$

**Proof.** Suppose that a solution exists for the Stefan problem with $(c^{\text{part}} - c^0)(c^{\text{part}} - c^{\text{sol}}) < 0$. We then have $c^0 < c^{\text{part}} < c^{\text{sol}}$, or $c^{\text{sol}} < c^{\text{part}} < c^0$.

First we consider the case that $c^0 < c^{\text{part}} < c^{\text{sol}}$. From the maximum principle we then have $\partial c/\partial v > 0$. From Eq. (14) and $(c^{\text{sol}} - c^0)\partial c/\partial v > 0$, follows that $v_v < 0$ and thus the particle grows. For $t = 0$, we have the relation

$$\int_{\Omega(0)\cup P(0)} (c(\underline{r}, 0) - c^0)\,\mathrm{d}r = (c^{\text{part}} - c^0)\int_{P(0)} \mathrm{d}V.$$

For $t > 0$, the difference is given by

$$\begin{aligned}\int_{\Omega(t)\cup P(t)} (c(\underline{r},t) - c^0)\,\mathrm{d}V &= (c^{\mathrm{part}} - c^0)\int_{P(t)} \mathrm{d}V + \int_{\Omega(t)} (c(\underline{r},t) - c^0)\,\mathrm{d}V \\ &= (c^{\mathrm{part}} - c^0)\left(\int_{P(0)} \mathrm{d}V + \int_{P(t)\setminus P(0)} \mathrm{d}V\right) + \int_{\Omega(t)} (c(\underline{r},t) - c^0)\,\mathrm{d}V \\ &= (c^{\mathrm{part}} - c^0)\int_{P(0)} \mathrm{d}V + \int_{\Omega(0)} (c(\underline{r},t) - c^0)\,\mathrm{d}V.\end{aligned}$$

From the maximum principle, it follows that $c(\underline{r},t) \geqslant c^0,\ \underline{r} \in \Omega(0)$. It is then clear that above equation implies

$$\int_{\Omega(t)\cup P(t)} (c(\underline{r},t) - c^0)\,\mathrm{d}V > (c^{\mathrm{part}} - c^0)\int_{P(0)} \mathrm{d}V. \tag{17}$$

Since $c$ is a solution of the Stefan problem it satisfies (16). However (17) implies that (15) is not valid. Thus Eqs. (16) and (15) are not equivalent, and hence according to Definition 3.1, the solution is not conserving. The Stefan problem with $c^0 < c^{\mathrm{part}} < c^{\mathrm{sol}}$ is therefore ill-posed. A similar proof can be given to show that for the case $c^{\mathrm{sol}} < c^{\mathrm{part}} < c^0$ no conserving solution exists either.

Suppose that a solution exists for the Stefan problem with $(c^{\mathrm{part}} - c^0)(c^{\mathrm{part}} - c^{\mathrm{sol}}) = 0$, then we either have $c^{\mathrm{part}} = c^0$ or $c^{\mathrm{part}} = c^{\mathrm{sol}}$. For the first case a similar proof as the preceding one can be used to show that no conserving solution exists. For the second case one can prove that $|v_v(t)|$ blows up because $\partial c(S(t),t)/\partial v \neq 0$ due to the maximum principle when $c^{\mathrm{sol}} \neq c^0$ (note the requirements on continuity of $c$). □

This proposition has been proved for a one-dimensional unbounded Stefan problem in [35].

If we have $(c^{\mathrm{part}} - c^0)(c^{\mathrm{part}} - c^{\mathrm{sol}}) > 0$, we either have $(c^{\mathrm{part}} < c^0) \wedge (c^{\mathrm{part}} < c^{\mathrm{sol}})$ or $(c^{\mathrm{part}} > c^0) \wedge (c^{\mathrm{part}} > c^{\mathrm{sol}})$. Then it can be proved in a similar way that a conserving solution is possible and we then call the Stefan problem well-posed. Furthermore, it appears that we will have dissolution, i.e. $v_v > 0$, if $(c^{\mathrm{sol}} - c^0)(c^{\mathrm{sol}} - c^{\mathrm{part}}) < 0$ and contrarily for the other well-posed problems, we will have growth. When the interface concentrations $c_{i,k}^{\mathrm{sol}}$ are constant the solution of the vector valued Stefan problem is called conserving when $(c_{i,k}^{\mathrm{part}} - c_i^0)(c_{i,k}^{\mathrm{part}} - c_{i,k}^{\mathrm{sol}}) > 0$ for all $i$ and $k$.

We expect that for a Stefan problem only conserving solutions occur. However, in the following sections we approximate the solution of a vector-valued Stefan problem. Due to the nonlinear boundary conditions the approximate solution is not unique. Therefore, we use the necessary condition given in this section to select a conserving solution. In our applications in metallurgy (where $c_{i,k}^{\mathrm{part}} \gg c_{i,k}^{\mathrm{sol}}$ for all $i$ and $k$) the conserving solution appears to be unique.

## 4. A self-similar solution for a planar vector-valued Stefan problem

Consider a planar particle dissolving in an infinite domain: $\Omega(t) := \{r \in \mathbb{R} | S(t) < r < \infty\}$. The function $c_i$ satisfies

$$\frac{\partial c_i}{\partial t} = \mathbb{D}_i \frac{\partial^2 c_i}{\partial r^2}, \quad r \in \Omega(t),\ t \in (0,T],\ i \in \{1,\ldots,n\}.$$

At the interface, we define: $c_i(S(t),t) =: c_i^{\mathrm{sol}}(t)$, $i \in \{1,\dots,n\}$. Furthermore, we assume for $t = 0$: $c_i(r,0) = c_i^0$, and $\lim_{r\to\infty} c_i(r,t) = c_i^0$, $i \in \{1,\dots,n\}$, where $c_i^0$ are given constants and $S(0) = S_0$.

It can be proved that the solution is [42,35]

$$c_i(r,t) = \frac{c_i^0 - c_i^{\mathrm{sol}}}{\mathrm{erfc}(k/2\sqrt{\mathbb{D}_i})}\mathrm{erfc}\left(\frac{r - S_0}{2\sqrt{\mathbb{D}_i t}}\right) + c_i^0, \quad r \in \Omega(t),\ t \in (0,T],\ i \in \{1,\dots,n\}, \tag{18}$$

where $k$ is defined in: $S(t) = S_0 + k\sqrt{t}$. Due to condition (8), the value of $k$ is independent of the chemical elements. Combination of (18) with (7) yields the following set of equations to be solved for $k$ and $c_i^{\mathrm{sol}}$ for all chemical elements:

$$\frac{k}{2} = \frac{c_i^0 - c_i^{\mathrm{sol}}}{c_i^{\mathrm{part}} - c_i^{\mathrm{sol}}}\sqrt{\frac{\mathbb{D}_i}{\pi}}\frac{\exp(-k^2/4\mathbb{D}_i)}{\mathrm{erfc}(k/2\sqrt{\mathbb{D}_i})}, \quad \forall i \in \{1,\dots,n\}, \tag{19}$$

$$\prod_{i=1}^{n}(c_i^{\mathrm{sol}})^{m_i} = K. \tag{20}$$

For the scalar Stefan problem this has been analyzed in [35]. We solve system (19) and (20) of $n+1$ nonlinear equations for $n+1$ variables ($k$, $c_i^{\mathrm{sol}}$, $i \in \{1,\dots,n\}$) with a numerical method. It turns out that the value of $k$ in the above equation can be approximated by

$$\tilde{k} = 2\frac{c_i^0 - c_i^{\mathrm{sol}}}{c_i^{\mathrm{part}} - c_i^{\mathrm{sol}}}\sqrt{\frac{\mathbb{D}_i}{\pi}} \tag{21}$$

provided that $|(c_i^0 - c_i^{\mathrm{sol}})/(c_i^{\mathrm{part}} - c_i^{\mathrm{sol}})| \ll 1$, for an $i \in \{1,\dots,n\}$. The value $\tilde{k}$ leads to the same solution as one would obtain from a (inverse) Laplace transform of the diffusion equation [43,1]. Before we state the accuracy of $\tilde{k}$, we define: $A_i := (c_i^0 - c_i^{\mathrm{sol}})/(c_i^{\mathrm{part}} - c_i^{\mathrm{sol}})\sqrt{1/\pi}$, $x_i := k/2\sqrt{\mathbb{D}_i}$, $f(x) := (\exp(-x^2)/\mathrm{erfc}(x))$. It turns out that approximation (21) represents a lower limit for the value of $k$. This is formulated in the following proposition.

**Proposition 4.1.** *Let $x_i/A_i = f(x_i)$ for a given, fixed $A_i < 1/\sqrt{\pi}$ then,*

$$A_i < x_i < \frac{A_i}{1 - \sqrt{\pi}A_i} \quad \textit{which implies } \tilde{k} < k < \frac{\tilde{k}}{1 - \sqrt{\pi}A_i}.$$

**Proof.** Using a series expansion of $f(x)/x$ at $x \to \infty$ [35], one obtains $\lim_{x\to\infty} f(x)/x = \sqrt{\pi}$. Furthermore, it is easy to see that $\lim_{x\to-\infty} f(x) = 0$. Since $f(x)$, $f'(x)$, $f''(x) > 0$, $x \in \mathbb{R}$ ($f$ is convex and monotonously increasing), one obtains: $0 < f'(x) < \sqrt{\pi}$, $x \in \mathbb{R}$. With $f(0) = 1$ and from the Mean Value Theorem $x_i/A_i = f(x_i) = 1 + x_i f'(\tilde{x}_i)$, $\tilde{x}_i \in (0, x_i)$, one obtains: $1 < x_i/A_i < 1 + \sqrt{\pi}x_i$ for $A_i \geqslant 0$. For $A_i < 0$ the inequality $1 + \sqrt{\pi}x_i < x_i/A_i < 1$ holds. Both inequalities lead to

$$A_i < x_i < \frac{A_i}{1 - A_i \cdot \sqrt{\pi}}. \qquad \square$$

Note that the proposition agrees with the requirement of well-posedness as discussed in Section 3. Moreover the proposition implies that $x_i A_i > 0$ when $x_i \neq 0$. When we insert the concentrations

into the definitions, one obtains from the proposition

$$S_0 + 2\frac{c_i^0 - c_i^{\mathrm{sol}}}{c_i^{\mathrm{part}} - c_i^{\mathrm{sol}}}\sqrt{\frac{\mathbb{D}_i t}{\pi}} < S_0 + k\sqrt{t} < S_0 + 2\frac{c_i^0 - c_i^{\mathrm{sol}}}{c_i^{\mathrm{part}} - c_i^0}\sqrt{\frac{\mathbb{D}_i t}{\pi}}. \tag{22}$$

From inequality (22), the velocity of the moving boundary can be bounded by

$$\frac{c_i^0 - c_i^{\mathrm{sol}}}{c_i^{\mathrm{part}} - c_i^{\mathrm{sol}}}\sqrt{\frac{\mathbb{D}_i}{\pi t}} < \frac{\mathrm{d}S(t)}{\mathrm{d}t} < \frac{c_i^0 - c_i^{\mathrm{sol}}}{c_i^{\mathrm{part}} - c_i^0}\sqrt{\frac{\mathbb{D}_i}{\pi t}}. \tag{23}$$

This (approximate) solution (21) will be used in the remainder of the present paper as a solution of the vector-valued Stefan problem since it gives a good insight into the asymptotic behavior of the solution. It is also noted that this lower bound would be obtained if the interface would be stationary, i.e. not moving [43]. Since the lower bound is only valid for the case that $A_i$ is sufficiently small, one must be careful in its use. Otherwise, the lower bound then may yield solutions that are not conserving (see Section 3 and [34]).

In real applications the distance between cells may be small. For these cases we have to deal with the fact that the domain is bounded. It can be proved [33] that for $c_{\mathrm{sol}} > c^0 \geqslant 0$ the solution $(c)$ in the bounded domain is larger than the solution in an infinite domain. This implies that the rate of dissolution is larger in an unbounded domain than in a bounded domain.

## 5. A limit solution for a planar vector valued Stefan problem

In this section we consider the consequences of the inequalities given in (23). For this purpose, we take the special situation that

- $c_i^{\mathrm{part}} \gg c_i^{\mathrm{sol}} > c_i^0 = 0,\ \forall i \in \{1,\ldots,n\}$.
  Since in metallurgy one often encounters $c_i^{\mathrm{part}} \gg c_i^{\mathrm{sol}} > c_i^0 \approx 0$, the solution that satisfies the above-mentioned constraints is referred to as a limit. From the inequalities we see that:
- $-1 \ll \frac{c_i^0 - c_i^{\mathrm{sol}}}{c_i^{\mathrm{part}} - c_i^{\mathrm{sol}}} < 0$,
- $\frac{c_i^0 - c_i^{\mathrm{sol}}}{c_i^{\mathrm{part}} - c_i^{\mathrm{sol}}} \approx -\frac{c_i^{\mathrm{sol}}}{c_i^{\mathrm{part}}}$.

From this and Eq. (21), one easily can write down the following recurrent relationship:

$$\frac{-c_i^{\mathrm{sol}}}{c_i^{\mathrm{part}}}\sqrt{\mathbb{D}_i} \approx \frac{-c_{i+1}^{\mathrm{sol}}}{c_{i+1}^{\mathrm{part}}}\sqrt{\mathbb{D}_{i+1}}, \quad \forall i \in \{1,\ldots,n-1\}. \tag{24}$$

Assuming an equality in Eq. (24) yields an approximate $\tilde{c}_i^{\mathrm{sol}}$:

$$\tilde{c}_i^{\mathrm{sol}} = \sqrt{\frac{\mathbb{D}_1}{\mathbb{D}_i}}\frac{c_i^{\mathrm{part}}}{c_1^{\mathrm{part}}}\tilde{c}_1^{\mathrm{sol}}. \tag{25}$$

Substitution of Eq. (25) into the assumption that $\prod_{i=1}^n (c_i^{\mathrm{sol}})^{m_i} = K$ and defining $\mu := \sum_{i=1}^n (m_i)$, one obtains

$$\left(\frac{\sqrt{\mathbb{D}_1}}{c_1^{\mathrm{part}}}\right)^{\mu} \prod_{i=1}^{n} \left(\frac{c_i^{\mathrm{part}}}{\sqrt{\mathbb{D}_i}}\right)^{m_i} (\tilde{c}_1^{\mathrm{sol}})^{\mu} = K. \tag{26}$$

The solution to Eq. (26) is

$$\tilde{c}_1^{\mathrm{sol}} = \frac{c_1^{\mathrm{part}}}{\sqrt{\mathbb{D}_1}} K^{\frac{1}{\mu}} \prod_{i=1}^{n} \left( \frac{\sqrt{\mathbb{D}_i}}{c_i^{\mathrm{part}}} \right)^{m_i/\mu}. \tag{27}$$

Substitution of the real, positive solution as given in Eq. (27) into Eq. (21) and using $S'(t) = k/2\sqrt{t}$, yields

$$\frac{\mathrm{d}S(t)}{\mathrm{d}t} \approx -\frac{c_{\mathrm{eff}}^{\mathrm{sol}}}{c_{\mathrm{eff}}^{\mathrm{part}}} \sqrt{\frac{\mathbb{D}_{\mathrm{eff}}}{\pi t}} \tag{28}$$

with $c_{\mathrm{eff}}^{\mathrm{sol}}$, $c_{\mathrm{eff}}^{\mathrm{part}}$ and $\mathbb{D}_{\mathrm{eff}}$ defined as: $c_{\mathrm{eff}}^{\mathrm{sol}} := K^{1/\mu}$, $c_{\mathrm{eff}}^{\mathrm{part}} := \prod_{i=1}^{n} (c_i^{\mathrm{part}})^{m_i/\mu}$, and $\mathbb{D}_{\mathrm{eff}} := \prod_{i=1}^{n} (\mathbb{D}_i)^{m_i/\mu}$. The symbols $c_{\mathrm{eff}}^{\mathrm{sol}}$, $c_{\mathrm{eff}}^{\mathrm{part}}$, and $\mathbb{D}_{\mathrm{eff}}$ are referred to as, respectively, the effective solid solubility, effective particle concentration and effective diffusion coefficient. We thus have approximated the solution to a vector-valued Stefan problem with a solution to a scalar Stefan problem. In other words the dissolution of a multi-component particle can be described by the dissolution of a particle in a quasi-binary alloy, where the effective particle concentration and effective diffusion coefficient are given by a geometrical mean of all particle concentrations and diffusion coefficients involved. One can integrate Eq. (28) in time to yield

$$S(t) \approx S_0 - 2\frac{c_{\mathrm{eff}}^{\mathrm{sol}}}{c_{\mathrm{eff}}^{\mathrm{part}}} \sqrt{\frac{\mathbb{D}_{\mathrm{eff}} t}{\pi}}. \tag{29}$$

This case holds for the assumptions that the particle concentrations are much larger than the concentrations at the moving boundary. Moreover, the initial concentrations in the primary phase has to be equal to zero. Nevertheless, Eq. (28) gives a good insight into the influence of the addition of an alloying element to the dissolution kinetics. The approximation may be used to test the results from the more general numerical solution. For the case in which the particle concentrations of all alloying elements are equal, i.e. $c_i^{\mathrm{part}} = c^{\mathrm{part}}$ and $m_i = 1$, $\forall i \in \{1, \ldots, n\}$, one can simplify the effective quantities to yield for this very special case:

$$c_{\mathrm{eff}}^{\mathrm{sol}} := (K)^{1/n}, \quad c_{\mathrm{eff}}^{\mathrm{part}} := c^{\mathrm{part}}, \quad \mathbb{D}_{\mathrm{eff}} := \left( \prod_{i=1}^{n} \mathbb{D}_i \right)^{1/n}.$$

It can now be seen that the effective diffusion coefficient is equal to the geometric mean of all the diffusion coefficients of the alloying elements.

To clarify this quasi-binary approach we compare this approach to the more general approach as described in Section 4. We take the following hypothetic quantities: $c_i^0 = 0$, $c_i^{\mathrm{part}} = 33\,\mathrm{mol/m^3}$, $\mathbb{D}_i = i \times 10^{-3}$ and $m_i = 1$, for $i \in \{1, 2, 3\}$ and $S_0 = 0.1$. From the approach as described in this section, one obtains for the effective values: $\mathbb{D}_{\mathrm{eff}} = 2.449510^{-3}$, $c_{\mathrm{eff}}^{\mathrm{part}} = 33$, $c_{\mathrm{eff}}^{\mathrm{sol}} = 1$, which yields: $S(t) = S_0 - 0.15 \times 10^{-2}\sqrt{t}$. Using the more general approach from Section 4 and Eqs. (19) and (20), one obtains as a solution: $S(t) = S_0 - 0.16 \times 10^{-2}\sqrt{t}$. The difference between the two solutions is small. The approximate solution gives a good order of magnitude for the dissolution kinetics.

## 6. The numerical method for vector-valued Stefan problems

Various numerical methods are known to solve Stefan problems: front-tracking, front-fixing, and fixed-domain methods [10]. In a front-fixing method a transformation of co-ordinates is used (a special case is the isotherm migration method (IMM)). Fixed-domain methods are the enthalpy method (EM) and the variational inequality method (VI). Various methods are compared in [11]. The latter methods (IMM, EM, VI) are only applicable when the concentration is constant at the interface. Since in our problem the concentration varies at the interface we restrict ourselves to a front-tracking method. Front-tracking methods are described in [24,3,19,44,4,45,17]. Recently a number of promising methods are proposed for multi-dimensional Stefan problems: phase field methods [6,7,41] and level set methods [22,29,9].

Our main interest is to give an accurate discretization of the boundary conditions for a one-dimensional Stefan problem. Therefore, we use the classical moving grid method of Murray and Landis [24] to discretize the diffusion equations. First an outline of the numerical method is given. In the present paper we generalize the method from [34] to a method which can be used for vector-valued Stefan problems.

The equations are solved with a finite difference method in the $r$- and $t$-direction. A characteristic feature of a front-tracking method is that the interface positions are nodal points in every time step. So, the position of the grid points depends on time. An outline of the algorithm is:

1. Compute the concentration profiles solving the nonlinear problem given by (1)–(6), (8),
2. Predict the positions of $S_L$ and $S_R$ at the new time step: $S_L(t+\Delta t)$ and $S_R(t+\Delta t)$,
3. Redistribute the grid such that $S_L(t+\Delta t)$ and $S_R(t+\Delta t)$ are nodal points. Use linear interpolation to approximate the concentrations at the previous time step on the new grid points,
4. Return to step 1.

### 6.1. Discretization of the interior region

In [34] the method is explained using an equidistant grid. For efficiency reasons we use a nonequidistant grid to solve vector-valued Stefan problems. The motivation for this is: from theory and numerical experiments it appears that the absolute values of the concentration gradients of the diffusing alloying elements are maximal at the moving boundaries. As the displacement of a free boundary is proportional to the concentration gradient the space discretization in the neighborhood of this boundary should be very accurate. Therefore a fine discretization grid is chosen near the free boundaries and a coarse grid farther away. A geometrically distributed grid is chosen. As an example consider one free boundary ($S_R(t) = M_R,\ t \in [0,T]$). The grid is distributed such that $\Delta r_l^{j+1} = \beta \Delta r_{l+1}^{j+1}$, with $\beta \leqslant 1$ and $\Delta r_l^{j+1} := r_{l+1}^{j+1} - r_l^{j+1}$. The resulting discretized equation for one alloying element is given by (for ease of notation we omit here the index $i$)

$$\frac{c_l^{j+1}}{\mathbb{D}\Delta t} + \left\{ (r_{l+\frac{1}{2}}^{j+1})^a \frac{c_{l+1}^{j+1} - c_l^{j+1}}{\Delta r_l^{j+1}} - (r_{l-\frac{1}{2}}^{j+1})^a \frac{c_l^{j+1} - c_{l-1}^{j+1}}{\Delta r_{l-1}^{j+1}} \right\} \Big/ \{ (r_l^{j+1})^a (\Delta r_l^{j+1}/2 + \Delta r_{l-1}^{j+1}/2) \}$$
$$= \frac{1}{\mathbb{D}\Delta t} \left\{ c_l^j + \frac{c_{l+1}^j - c_{l-1}^j}{\Delta r_l^{j+1} + \Delta r_{l-1}^{j+1}} (r_l^{j+1} - r_l^j) \right\}, \tag{30}$$

where $c_l^j$ approximates the concentration $c(r_l^j,\ j\Delta t)$. For more details we refer to [31, pp. 255–261].

### 6.2. Discrete boundary condition at a moving boundary

For the case of two moving boundaries, i.e. $M_L < S_L(t)$ and $S_R(t) < M_R$, $t \in [0,T]$, the solutions of the diffusion equations are formally determined by the concentrations of all alloying elements at the boundaries $S_L$ and $S_R$. So a change of a concentration at $S_L$ influences the solution of the diffusion equations and hence the gradients of concentration at $S_R$ (and vice versa). However, it has been shown in [34] that for $\Delta t$ sufficiently small the concentrations at $(j+1)\Delta t$ in the vicinity of $S_L$ are not influenced by the concentrations at $(j+1)\Delta t$ in the vicinity of $S_R$. An explanation is given using the theory of penetration. In most applications $\Delta t$ is already chosen less than this bound for accuracy reasons. So in this section we assume that the boundary conditions on both moving boundaries are independent.

The boundary conditions are discretized with virtual grid points. The virtual concentrations are eliminated by (30). For ease of notation we only consider $S_L$ and assume that $\Phi_L = \{1,\dots,n\}$ and $S_R(t) = M_R$. All concentrations which satisfy (30) and the boundary conditions on $M_R$ are functions of $c_{i,0}^{j+1}$, $i \in \{1,\dots,n\}$, which is the concentration of alloying element $Sp_i$ at $S_L$. To determine these remaining unknowns one has to solve the following nonlinear equations:

$$f_i(c_{i,0}^{j+1}, c_{i+1,0}^{j+1}) := \mathbb{D}_i(c_{i+1}^{\text{part}} - c_{i+1,0}^{j+1})(c_{i,1}^{j+1} - c_{i,-1}^{j+1}) - \mathbb{D}_{i+1}(c_i^{\text{part}} - c_{i,0}^{j+1})(c_{i+1,1}^{j+1} - c_{i+1,-1}^{j+1}) = 0 \tag{31}$$

for $i \in \{1,...,n-1\}$ and

$$f_n(c_{1,0}^{j+1},\dots,c_{n,0}^{j+1}) := \prod_{i=1}^{n}(c_{i,0}^{j+1})^{m_i} - K_L = 0. \tag{32}$$

To approximate a root for the vector function $(f_1,...,f_n)^{\mathrm{T}}$ we use the Newton–Raphson method:

$$\begin{pmatrix} c_{1,0}^{j+1}(p+1) \\ \vdots \\ c_{n,0}^{j+1}(p+1) \end{pmatrix} = \begin{pmatrix} c_{1,0}^{j+1}(p) \\ \vdots \\ c_{n,0}^{j+1}(p) \end{pmatrix} + (J(p))^{-1} \cdot \begin{pmatrix} -f_1(p) \\ \vdots \\ -f_n(p) \end{pmatrix}, \tag{33}$$

where $J$ is the Jacobian and the $p$th iterate of the concentration is denoted by $c_{i,0}^{j+1}(p)$. The matrix $J$ is sparse. Only the matrix elements of the last row and the elements $J_{i,i}$ and $J_{i,i+1}$, $i \in \{1,\dots,n-1\}$ are nonzero. In practice, it is impossible to compute the first $n-1$ rows of $J$. Therefore we use a discrete approximation $\hat{J}$. The elements of $\hat{J}$ are obtained from

$$\hat{J}_{i,i} = [f_i(c_{i,0}^{j+1} + \varepsilon, c_{i+1,0}^{j+1}) - f_i(c_{i,0}^{j+1} - \varepsilon, c_{i+1,0}^{j+1})]/2\varepsilon, \quad i \in \{1,\dots,n-1\},$$

$$\hat{J}_{i,i+1} = [f_i(c_{i,0}^{j+1}, c_{i+1,0}^{j+1} + \varepsilon) - f_i(c_{i,0}^{j+1}, c_{i+1,0}^{j+1} - \varepsilon)]/2\varepsilon, \quad i \in \{1,\dots,n-1\}.$$

Note that $\varepsilon$ has to be sufficiently small, but larger than the accuracy of the numerical scheme to evaluate the concentrations. The computation of $\hat{J}$ requires that in every Newton–Raphson iteration the discretized equations have to be solved $2(n-1)$ times (also when $S_R(t) < M_R$).

To start the Newton–Raphson procedure an initial guess has to be found. To prevent convergence to an undesired root, the initial guess is chosen as close as possible to the root. For time-steps $j > 1$,

the boundary concentrations from the former time step are chosen as initial guesses. However, at time step $j = 1$, the analytical approximations are used. We terminate the iteration when

$$\sum_{i=1}^{n} |c_{i,0}^{j+1}(p+1) - c_{i,0}^{j+1}(p)| < \varepsilon.$$

### 6.3. Adaptation of the moving boundaries

We have not used all boundary conditions given in (7) to determine the concentrations. The remaining conditions are used to adapt the positions of the moving boundaries. In [34] the Euler Forward and Trapezium time integration methods are described to determine the moving boundary positions. The Trapezium method is preferred because the costs per iteration are the same for both methods, but the results obtained with the Trapezium method are more accurate [34]. For the solution of a vector-valued Stefan problem we have implemented the Trapezium integration method iteratively, simultaneously with the Newton–Raphson iteration to obtain $c_{i,0}^{j+1}$. The iteration is terminated when

$$\sum_{i\in\Phi_L} |c_{i,0}^{j+1}(p+1) - c_{i,0}^{j+1}(p)| + \frac{|S_L^{j+1}(p+1) - S_L^{j+1}(p)|}{S_L^j - M_L} < \varepsilon.$$

## 7. Numerical experiments

This section contains some numerical experiments. Experiments to test the accuracy of the numerical calculations have been omitted. Here we remark only that the accuracy of the time integration was order $\Delta t$ and the accuracy of the mesh size was order $\Delta r^2$. For stability reasons we took $\Delta t < 1000(\Delta r^2/\max(\mathbb{D}_i))$. We refer to [34] for more details. First we compare the solutions obtained with the numerical method, as described in Section 6 with the solutions from the analytical relations of Sections 4 and 5. We also show the behavior of the concentration profile of the alloying elements. Finally, we show an example of an application of the model in aluminum industry.

### 7.1. A comparison between the numerical and analytical solutions

The first example treats a system in which the analytical results do not differ very much. We have set: $c_i^{\text{part}} = 100$, $c_i^0 = 0$, $\mathbb{D}_i = i \times 10^{-13}$, $i \in \{1,2,3\}$, $K = 1$, $S_L(0) = 0.1 \times 10^{-6}$ m. For the finite distance, we set $S_R(0) = M_R = 0.1 \times 10^{-4}$ m. Where we imposed an homogeneous Neumann condition. The position of the moving boundary, $S(t)$, has been sketched as a function of time in Fig. 2. In this figure we also present three analytical curves: the analytical solution obtained from Eqs. (19) and (20) and both the upper and lower bounds for the dissolution kinetics as given in Eq. (22) (Fig. 3). It can be seen that the analytical curves hardly differ. This is because $c_i^{\text{part}} \gg c_i^{\text{sol}}$. It can also be seen that the results from the numerical approach matches perfectly with the results from the analytical approaches at the early stages. However, at the later stages, from $t > 150$, the approaches start to differ significantly. This is due to the fact that the primary phase, in which we have diffusion, starts to saturate: the concentration profiles start to flatten. To illustrate this behavior, the concentration profiles of all the alloying elements have been sketched at $t = 50$ and 200, respectively, in Figs. 4 and 5. At $t = 50$ the concentration of the chemical elements at $M_R$ has hardly changed. Up to then,

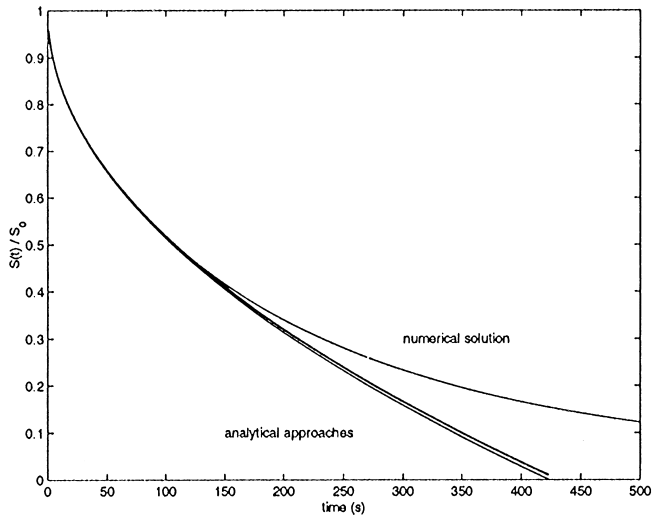


Fig. 2. The numerical and analytical results for $c_i^{\text{part}} = 100$.

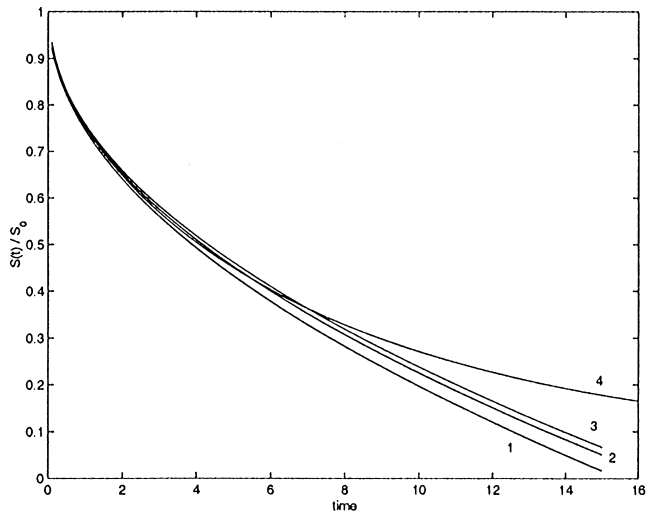


Fig. 3. ($c_i^{\text{part}} = 20$) Curve 1: lower bound, Curve 2: analytical solution, Curve 3: upper bound, Curve 4: numerical solution.

the numerical and analytical solutions match perfectly (see Fig. 2). It can be seen that at $t = 200$ the concentration of the alloying elements at $M_R$ starts to increase. The profiles flatten and the dissolution kinetics are delayed compared to the analytical approaches for the unbounded domain. This has been remarked before.

In the second example we maintained the settings of the first example except for the particle concentrations: $c_i^{\text{part}} = 20$, $i \in \{1, 2, 3\}$ and $M_R = 0.2 \times 10^{-5}$. The results have been sketched in Fig. 3. The analytical curves differ more than in the preceding example. The analytical solution falls just within the limits and so does the numerical solution initially. It can however, be seen that the

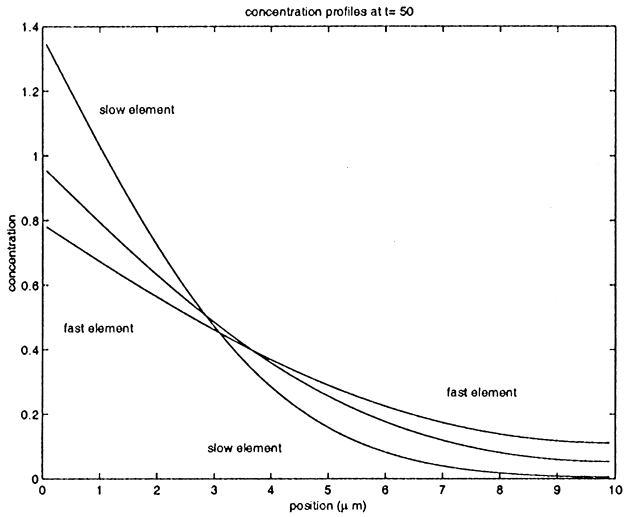


Fig. 4. Concentration profiles of the chemical elements at $t = 50$.

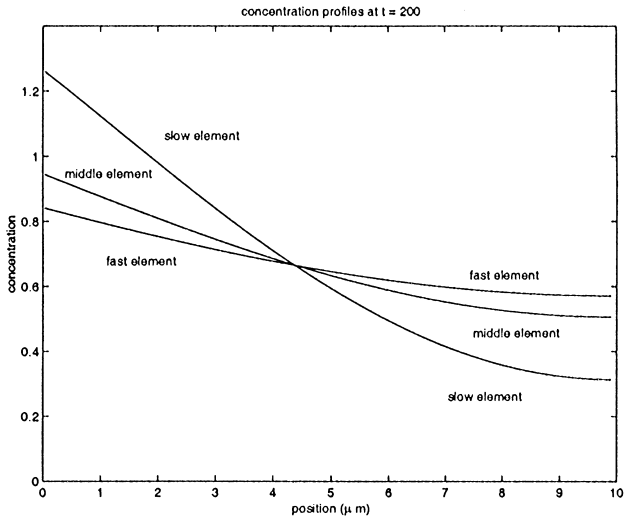


Fig. 5. Concentration profiles of the chemical elements at $t = 200$.

numerical approach and exact analytical approach for the unbounded domain differ a little at already early stages. This is attributed to the numerical inaccuracy. At the later stages it can be seen that the numerical and analytical solution start to deviate significantly. This is again attributed to the saturation of the primary phase. From the experiments it may be seen that the analytical curves provide a good order of magnitude for the dissolution kinetics as long as the concentration at the fixed boundary does not change significantly.

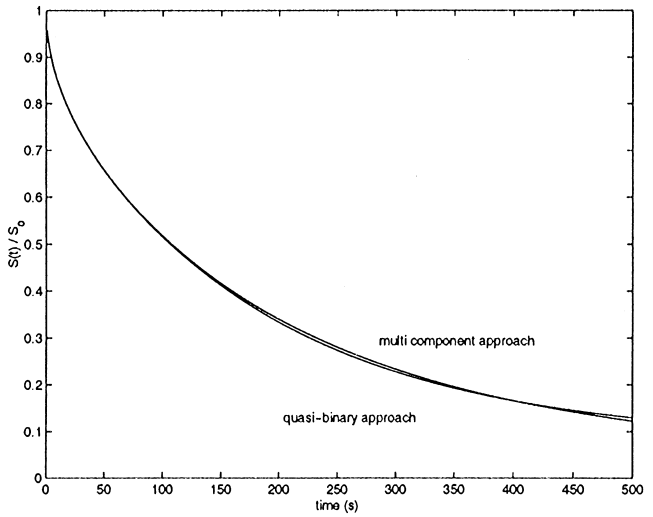


Fig. 6. The interface position as a function of time for a dissolving plane ($c_i^{\text{part}} = 100$).

### 7.2. The quasi-binary and multi-component approach compared

For the same two configurations as in the preceding subsection, we look at the quasi-binary and multi-component approach. With the quasi-binary approach, we mean the finite difference calculations, in which we incorporate the effects of the finite cell dimensions, done with the so-called effective diffusion coefficient, effective interface and particle concentration.

Fig. 6 presents the calculations done for the first case of the preceding subsection, i.e. the particle concentration is 100 for all chemical elements. It can be seen that the difference between the quasi-binary and multi-component approach is negligible. The same calculations have been done for the case that the particle concentration is 20 for all chemical elements. The results are shown in Fig. 7. As can be expected from the theory, the difference between the calculations is larger now. Nevertheless, the calculations, still do provide a good order of magnitude. This quasi-binary approach may be used to test the numerical calculations for the multi-component algorithm for cases in which the cell radius is not large. Moreover, the quasi-binary approach can be used well as an engineering solution for the case that no multi-component algorithm is available or to save CPU-time.

For completeness it is noted that all the theory about the quasi-binary approach is only valid for the case that the geometry is planar, although we expect that it is also a suitable approach for other geometries.

### 7.3. A spherical example with five alloying elements

An example of an application of the model to five alloying elements is given in Fig. 8. Figure 8 displays the interface position as a function of time for a spherical geometry. We chose $c_i^{\text{part}} = 20$, $S_L(0) = 1 \times 10^{-6}$, $S_R(0) = M_R = 5 \times 10^{-6}$ and $\mathbb{D}_i = i \times 10^{-13}$, $i \in \{1,\ldots,5\}$. It can be seen that the shape of the curve differs from the planar geometry. This difference is due to the curvature of the moving boundary: during dissolution the moving boundary area decreases, whereas this area

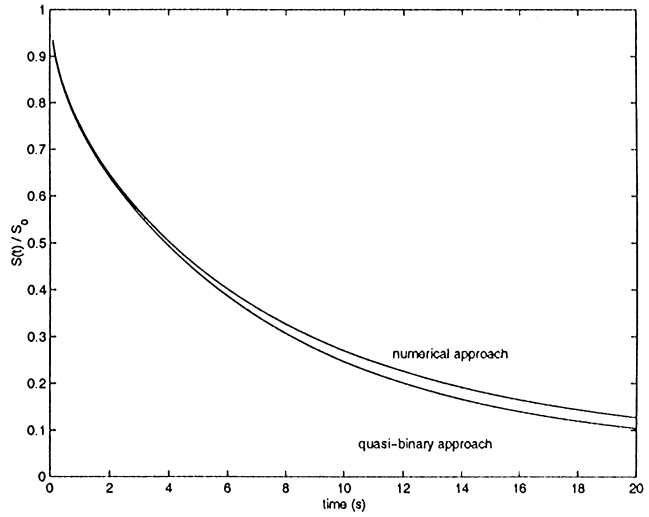


Fig. 7. The interface position as a function of time for a dissolving plane ($c_i^{\text{part}} = 20$).

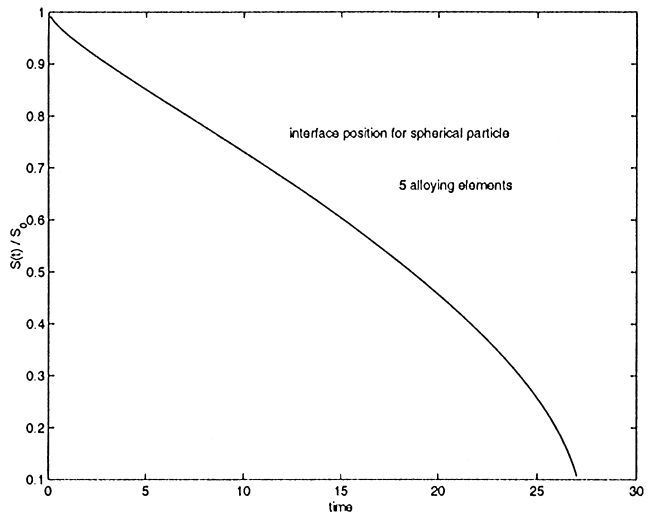


Fig. 8. The interface position as a function of time for a dissolving sphere with five alloying elements.

remains constant for the planar case. It may also be noted that the interface position does not assume a square-root-like behavior as in the case of a planar particle. This characteristic can be observed for cylindrical and spherical geometries. Another characteristic that can be observed for curvilinear geometries is the dependency of the interface concentrations on time (see Fig. 9). The increase of the interface concentrations is physically interpreted as an accumulation of the slower alloying elements on the interface. These slower alloying elements diffuse at a slower rate from the interface deeper into the primary phase.

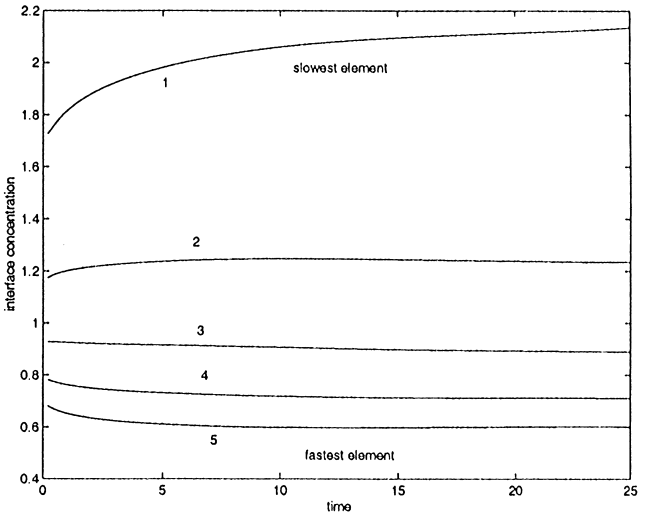


Fig. 9. The interface concentrations as a function of time.

### 7.4. An industrial example with a three-component system

As an industrial example of the mathematical model, we look at a three-component system. We consider the simultaneous dissolution of a Si-particle and a $Mg_2Si$-particle in an Al-alloy. The silicon particle is in the center of the spherical cell in which we consider the dissolution. The Si-particle is enclosed by the aluminum-rich phase (primary phase), which is enclosed by a $Mg_2Si$-phase. We also have incorporated a temperature–time profile, which is common in aluminum industry. The alloy is heated from 300 up to 823 K with a heat-up rate of 0.05 K/s. The initial concentration in the primary phase is: $c^0_{\mathrm{Si}} = 0$, $c^0_{\mathrm{Mg}} = 0.04$, whereas the particle concentrations are given by: $c^{\mathrm{part}}_{\mathrm{Si},L} = 100$, $c^{\mathrm{part}}_{\mathrm{Si},R} = 35$ and $c^{\mathrm{part}}_{\mathrm{Mg},R} = 65$. For the diffusion coefficients of silicon and magnesium, we, respectively, have $\mathbb{D}_{\mathrm{Si}} = 2.02 \times 10^{-4}$ and $\mathbb{D}_{\mathrm{Mg}} = 0.49 \times 10^{-4}$. Then for the solubility product of silicon and magnesium in aluminum, we have $K = 4.03 \times 10^{-5} \cdot \exp(74488/8.3 \cdot \tau)$, in which $\tau$ is the temperature. For the solubility of silicon in aluminum, we have used the discrete data from [23].

We assume that no magnesium diffuses into the silicon particle, i.e. we impose an homogeneous Neumann condition for magnesium at boundary $S_L$. Due to the homogeneous Neumann condition at $S_L$, magnesium accumulates at this boundary. For the case that the concentration of magnesium at the boundary of the silicon particle ($S_L$) is low enough, one can use the solubility of silicon in pure aluminum, given by binary-phase diagrams. If, however, magnesium accumulates up to a certain threshold value, the concentration of silicon at the boundary $S_L$ has to satisfy the hyperbolic relationship of the solubility of silicon and magnesium in aluminum. In a more mathematical notation, we thus write for the silicon concentration at the boundary $S_L$:

$$c^{\mathrm{sol}}_{\mathrm{Si}} = \frac{K_{\mathrm{Mg_2Si}}}{c_{\mathrm{Mg}}(S_L(t),t)^2} \cdot H(c_{\mathrm{Mg}}(S_L(t),t) - \tilde{C}) + K_{\mathrm{Si}} \cdot H(\tilde{C} - c_{\mathrm{Mg}}(S_L(t),t)). \tag{34}$$

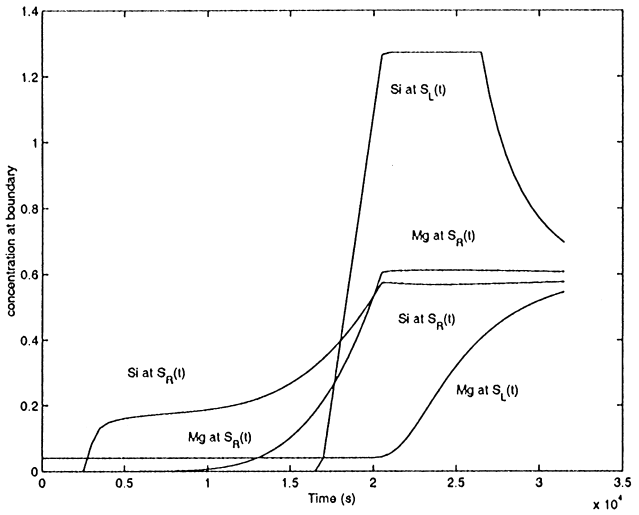


Fig. 10. The concentrations at the moving boundary as a function of time.

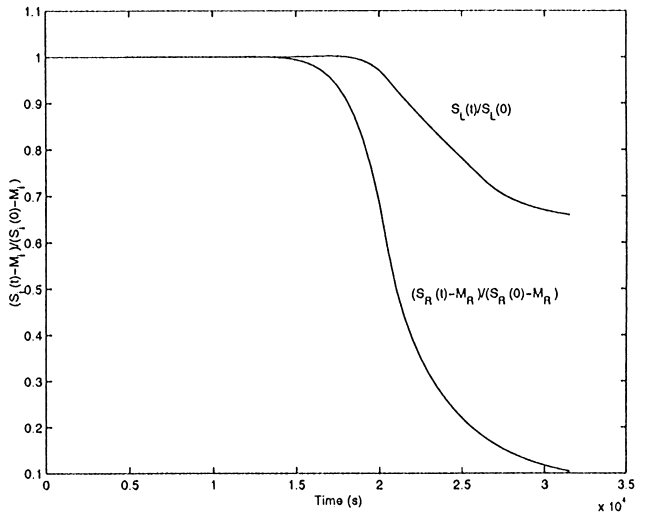


Fig. 11. The moving boundary positions as a function of time.

In which $H$ represents the heavy-side function and the threshold concentration $\tilde{C}$ follows from the continuity of the above relation (34), i.e.: $\tilde{C} = \sqrt{K_{Mg_2Si}/K_{Si}}$. Note that $K_{Mg_2Si}$ and $K_{Si}$ are functions of temperature and hence so is $\tilde{C}$. The results of the experiments with the simultaneous dissolution of an Si and $Mg_2Si$-particle are shown in Figs. 10 and 11.

It can be seen from Fig. 10 that both the silicon and magnesium concentration at the boundary $S_R$ increase with time. This is due to the temperature increase. When the temperature is constant (833 K, $t = 2.05 \times 10^4$), the concentrations at the boundary $S_R$ stay approximately constant. It can

also be seen that the silicon concentration at $S_L$ starts to increase very rapidly after approximately $1.6 \times 10^4$ s. Once the temperature is fixed, the Si-concentration at $S_L$ is fixed as well, until the magnesium concentration has passed the so-called threshold concentration $\tilde{C}$ (at $t = 2.7 \times 10^4$). The Si-concentration then starts to decrease according to Eq. (34). We only have shown the most interesting part of the calculation ($t \in (0, 3.1 \times 10^4]$). The evolution of the moving boundary positions is shown in Fig. 11. Note that due to the jump in the functional dependency in Eq. (34), the $S_L(t)$ may have a discontinuous time derivative.

## 8. Conclusions

A mathematical model is presented to describe the dissolution of stoichiometric multi-component particles in multi-component alloys.

A definition is introduced about conserving solutions to Stefan problems. It is proved in $\mathbb{R}^d$ for a scalar Stefan problem that no conserving solution exists if

$$(c^{\text{part}} - c^0)(c^{\text{part}} - c^{\text{sol}}) \leqslant 0, \quad c^{\text{sol}} \neq c^0 \quad \text{and} \quad c^0, c^{\text{sol}}, c^{\text{part}} \in \mathbb{R}^+ \cup \{0\}.$$

For a planar particle dissolving in an unbounded domain, a self-similar solution is given for the the dissolution of a multi-component particle. From the exact similarity solution two bounds have been derived for the dissolution of a planar particle in an unbounded domain. These bounds are easy to calculate and provide good insight into the dissolution kinetics and can therefore be used for engineering purposes as well.

For the case of initial concentrations equal to zero, a simple expression is derived for the dissolution in terms of an effective diffusion coefficient. It turns out that the effective diffusion coefficient is equal to a geometric mean of all diffusion coefficients involved. The weight factors come from the particle concentrations.

Finally, a numerical method is presented to deal with more general cases: cylindrical/spherical co-ordinates and two boundaries. It has been shown that the results of the numerical method agree well with the results obtained from the analytical approaches for the planar case as long as the solution at the fixed boundary did not change significantly from the initial condition.

## References

[1] H.B. Aaron, G.R. Kotler, Second phase dissolution, Metall. Trans. 2 (1971) 393–407.
[2] U.L. Baty, R.A. Tanzilli, R.W. Heckel, Dissolution kinetics of CuAl2 in an Al-4Cu alloy, Metall. Trans. 1 (1970) 1651–1656.
[3] R. Bonnerot, P. Jamet, A second order finite element method for the one-dimensional Stefan problem, Int. J. Numer. Methods Eng. 8 (1974) 811–820.
[4] K. Brattkus, D.I. Meiron, Numerical simulations of unsteady crystal growth, SIAM J. Appl. Math. 52 (1992) 1303–1320.
[5] M. Brokate, N. Kenmochi, I. Müller, J.F. Rodriguez, C. Verdi, Phase transitions and hysteresis; Lectures given at the 3rd Session of the Centro Internazionale Matematico Estivo (CIME) held in Montecatini Terme, Italy, July 13–21, 1993, Lecture Notes in Mathematics, Vol. 1584, Springer, Berlin, 1994.
[6] G. Caginalp, An analysis of a phase field model of a free boundary, Arch. Rat. Mech. Anal. 92 (1986) 205–245.
[7] G. Caginalp, J.T. Lin, A numerical analysis of an anisotropic phase field model, IMA J. Appl. Math. 39 (1987) 51–66.

[8] J. Chadam, H. Rasmussen, Free Boundary Problems Involving Solids, Longman Scientific & Technical, Harlow, 1993.
[9] S. Chen, B. Merriman, S. Osher, P. Smereka, A simple level set method for solving Stefan problems, J. Comput. Phys. 135 (1997) 8–29.
[10] J. Crank, Free and Moving Boundary Problems, Clarendon Press, Oxford, 1984.
[11] A.J. Dalhuijsen, A. Segal, Comparison of finite element techniques for solidification problems, Int. J. Numer. Methods Eng. 23 (1986) 1807–1829.
[12] F. Vermolen, C. Vuik, S. van der Zwaag, A mathematical model for the dissolution kinetics of $Mg_2Si$-phases in Al–Mg–Si alloys during homogenisation under industrial conditions, Mater. Sci. Eng. A 254 (1998) 13–32.
[13] A. Friedman, Partial Differential Equations of Parabolic Type, Prentice-Hall, Englewood Cliffs, NJ, 1964.
[14] J. Ågren, Diffusion in phases with several components and sublattices, J. Phys. Chem. Solids 43 (1981) 421–430.
[15] J.M. Hill, One-dimensional Stefan Problems: an Introduction, Pitman Monographs and Surveys in Pure and Applied Mathematics, Vol. 31, Longman Scientific & Technical, New York, 1987.
[16] R. Hubert, Modelisation numerique de la croissance et de la dissolution des precipites dans l'acier, ATB Metallurgie 34–35 (1995) 5–14.
[17] D. Juric, G. Tryggvason, A front-tracking method for dendritic solidification, J. Comput. Phys. 123 (1996) 127–148.
[18] J.S. Kirkaldy, D.J. Young, Diffusion in the Condensed State, The Institute of Metals, London, 1987.
[19] P. Lesaint, R. Touzani, Approximation of the heat equation in a variable domain with application to the Stefan problem, SIAM J. Numer. Anal. 26 (1989) 366–379.
[20] E. Magenes, C. Verdi, A. Visintin, Theoretical and numerical results on the two-phase Stefan problem, SIAM J. Numer. Anal. 26 (1989) 1425–1438.
[21] A.M. Meirmanov, The Stefan problem, De Gruyter Expositions in Mathematics, Vol. 3, Walter de Gruyter, Berlin, 1992.
[22] B. Merriman, J.K. Bence, S.J. Osher, Motion of multiple functions: a level set approach, J. Comput. Phys. 112 (1994) 334–363.
[23] L.F. Mondolfo, Aluminium Alloys, Structure and Properties, Butterworth, London, 1976.
[24] W.D. Murray, F. Landis, Numerical and machine solutions of transient heat-conduction problems involving melting or freezing, Trans. ASME (C) J. Heat Transfer 81 (1959) 106–112.
[25] F.V. Nolfi Jr., P.G. Shewmon, J.S. Foster, The dissolution and growth kinetics of spherical precipitates, Trans. Metall. Soc. AIME 245 (1969) 1427–1433.
[26] R.L. Parker, Crystal growth mechanisms: energetics, kinetics and transport, Solid State Phys. 25 (1970) 152–298.
[27] M.H. Protter, H.F. Weinberger, Maximum Principles in Differential Equations, Prentice-Hall, Englewood Cliffs, NJ, 1967.
[28] O. Reiso, N. Ryum, J. Strid, Melting and dissolution of secondary phase particles in AlMgSi-alloys, Metall. Trans. A 24A (1993) 2629–2641.
[29] J.A. Sethian, Level set methods; evolving interfaces in geometry, fluid mechanics, computer vision, and materials science, Cambridge Monographs on Applied and Computational Mathematics, Vol. 3, Cambridge University Press, Cambridge, 1996.
[30] U.H. Tundal, N. Ryum, Dissolution of particles in binary alloys: Part I, Computer simulations, Metall. Trans. 23A (1992) 433–449.
[31] F. Vermolen, Mathematical Models for Particle Dissolution in Extrudable Aluminium Alloys, Ph.D. Thesis, Delft University of Technology, The Netherlands, 1998.
[32] F.J. Vermolen, S. Van der Zwaag, A numerical model for the dissolution of spherical particles in binary alloys under mixed mode control, Mater. Sci. Eng. A 220 (1996) 140–146.
[33] F.J. Vermolen, C. Vuik, A mathematical model for the dissolution of particles in multi-component alloys, CWI-Report, MAS-R9822, 1998.
[34] F. Vermolen, C. Vuik, A numerical method to compute the dissolution of second phases in ternary alloys, J. Comput. Appl. Math. 93 (1998) 123–143.
[35] F. Vermolen, C. Vuik, A vector-valued Stefan problem from aluminium industry, Nieow Archiet voor Wiskunde, Vierde Serie 17 (2) (1999) 205–217.
[36] F Vermolen, C. Vuik, S. van der Zwaag, The dissolution of a stoichiometric second phase in ternary alloys: a numerical analysis, Mater. Sci. Eng. A A246 (1998) 93–103.

[37] A. Visintin, Models of Phase Transitions, Progress in Nonlinear Differential Equations and Their Application, Vol. 28, Birkhäuser, Boston, 1996.
[38] J.M. Vitek, S.A. Vitek, S.A. David, Modelling of diffusion controlled phase transformation in ternary systems and application to the Ferrite/Austenite transformation in the Fe-Cr-Ni-system, Metall. Trans. A 26A (1995) 2007–2025.
[39] C. Vuik, The Solution of a One-Dimensional Stefan Problem, Vol. 90, CWI-Tract, CWI-Amsterdam, 1993.
[40] C. Vuik, A. Segal, F.J. Vermolen, A conserving discretisation for a Stefan problem with an interface reaction at the free boundary, CWI-Report, MAS-R9904, 1999.
[41] S-L. Wang, R.F. Sekerka, Algorithms for phase field computation of the dentritic operating state at large supercoolings, J. Comput. Phys. 127 (1996) 110–117.
[42] H. Weber, Die Partiellen Differential-Gleichungen der Mathematischen Physik II, Vieweg, Braunschweig, 1901.
[43] M.J. Whelan, On the kinetics of particle dissolution, Metal Sci. J. 3 (1969) 95–97.
[44] D.E. Womble, A front-tracking method for multiphase free boundary problems, SIAM J. Numer. Anal. 26 (1989) 380–396.
[45] M. Zerroukat, C.R. Chatwin, Computational Moving Boundary Problems, Applied and Engineering Mathematics Series 8, Wiley, New York, 1994.